ELSEVIER

Pharmacological Research 56 (2007) 318–328

Pharmacological research

www.elsevier.com/locate/yphrs

Synthesis, *in vitro* activity and *in vivo* toxicity of the new 2,3-dinitrobutadiene derivative (1*E*,3*E*)-1,4-bis(2-naphthyl)-2,3-dinitro-1,3-butadiene

Maurizio Viale[a,*], Giovanni Petrillo[b], Cinzia Aiello[a], Carla Fenoglio[c], Cinzia Cordazzo[a], Maria A. Mariggiò[d], Amalia Cassano[d], Claudia Prevosto[e], Emanuela Ognio[f], Massimo Maccagno[b], Lara Bianchi[b], Rita Vaccarone[c], Egon Rizzato[g], Domenico Spinelli[g]

[a] *Istituto Nazionale per la Ricerca sul Cancro, S.C. Terapia Immunologica, L.go R. Benzi 10, 16132 Genova, Italy*
[b] *Dipartimento di Chimica e Chimica Industriale, Università di Genova, Via Dodecaneso 31, 16146 Genova, Italy*
[c] *Dipartimento di Biologia Animale, Università di Pavia, P.za Botta 10, 27100 Pavia, Italy*
[d] *Dipartimento di Scienze Biomediche e Oncologia Umana, Università di Bari, Osp. Policlinico, P.za G. Cesare 11, 70124 Bari, Italy*
[e] *Istituto Nazionale per la Ricerca sul Cancro, S.C. Oncologia Sperimentale D, L.go R. Benzi 10, 16132 Genova, Italy*
[f] *Istituto Nazionale per la Ricerca sul Cancro, S.S. Sperimentazioni su Modelli Animali, L.go R. Benzi 10, 16132 Genova, Italy*
[g] *Dipartimento di Chimica Organica "A. Mangini", Università di Bologna, Via San Giacomo 11, 40126 Bologna, Italy*

Accepted 31 July 2007

Abstract

Our interesting results on the antiproliferative (*in vitro*) and antitumour (*in vivo*) activities of (1*E*,3*E*)-1,4-bis(1-naphthyl)-2,3-dinitro-1,3-butadiene (1-Naph-DNB) have more recently induced us to design and synthesize some new 1,4-diaryl-2,3-dinitro-1,3-butadienes characterized by a common arylnitrobutadiene array but with different geometric and/or functional properties. This task was undertaken with the aim to obtain new compounds with an enhanced antiproliferative activity and, possibly, a different specificity with respect to the original (lead) compound. (1*E*,3*E*)-1,4-Bis(2-naphthyl)-2,3-dinitro-1,3-butadiene (2-Naph-DNB) is one of the molecules so obtained, a structural isomer of 1-Naph-DNB provided with a different spatial arrangement. When analyzed *in vitro* for its inhibition of cell proliferation 2-Naph-DNB showed a remarkable activity in the range of micromolar concentrations, with significant differences, with respect to 1-Naph-DNB, against some cell lines. Furthermore, it was able to significantly trigger apoptosis, to up-regulate p53, to block cells in the G2/M phase of the cell cycle and, finally, to slightly bind to DNA forming interstrand cross-links (ISCL).

2-Naph-DNB was then analyzed for its toxic activity *in vivo* in CD1 mice. This allowed the determination of toxicity parameters such as the lethal doses (LD) and the maximal tolerated dose (MTD) together with the definition of the spectrum of tissue alterations due to its administration i.v.

Altogether our data suggest that the idea of modifying the geometry of the lead compound 1-Naph-DNB deserves further investigation aimed at synthesizing new molecules with similar chemical functionalities but with different spatial requirements, hopefully characterized by still enhanced activities in terms of inhibition of cell proliferation and apoptosis.

Keywords: Naphthylnitrobutadienes; Antiproliferative activity; Apoptosis; Toxicity

1. Introduction

In spite of an intensive and capillary information about primary prevention, the increased risk of exposure to carcinogens due to the explosive progress of life conditions in developed countries and the consequent global environmental modifications have constantly and significantly increased the incidence

* Corresponding author. Tel.: +39 010 5737320.
E-mail address: maurizio.viale@istge.it (M. Viale).

1043-6618/$ – see front matter © 2007 Elsevier Ltd. All rights reserved.
doi:10.1016/j.phrs.2007.07.009

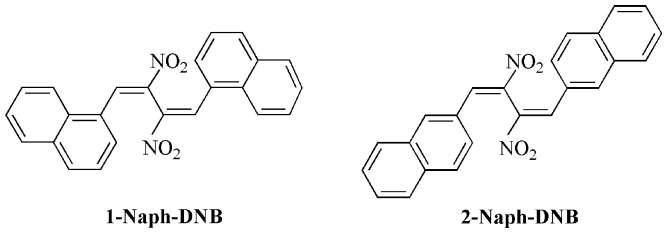

Fig. 1. Molecular structures of 1-Naph-DNB and 2-Naph-DNB.

of cancer (which is the main cause of mortality after cardiovascular diseases) in the last few years [1–4]. Many tumour histotypes, such as those of stomach, brain, pancreas, colorectum, and lung, have still a bad prognosis associated with an unacceptable high mortality. This is also because the range of chemotherapeutic weapons nowadays available does not yet cover all possible intrinsic or acquired forms of resistance to drugs [5–7].

Obviously, in these conditions the discover of new molecular structures endowed with significant antiproliferative activities and specificity against new tumour histotypes still remains an essential goal of pharmacological research [8,9].

In previous papers [10–13] we have reported on the antiproliferative activity *in vitro* and on the antitumour activity *in vivo* of 1-Naph-DNB (Fig. 1). This molecule showed a pharmacologically significant activity *in vitro* in terms of inhibition of cell proliferation, cytotoxicity and induction of apoptosis, together with a particular selectivity for cell lines derived from otherwise unresponsive gastrointestinal tumours. This last result was in part confirmed *in vivo* [13].

The enlightened ability of 1-Naph-DNB to form interstrand cross-links with the DNA of tumour cells as the most likely mechanism of apoptosis [10] has suggested the opportunity to consider its molecular structure as a prototype for the design of novel molecules in search for new and/or enhanced pharmacological activities in terms of intensity and specificity. Within this research line, we have now synthesized the isomeric 2-Naph-DNB (Fig. 1), characterized by the same chemical functionalities as 1-Naph-DNB [i.e. by the presence of a (1*E*,3*E*)-2,3-dinitro-1,3-butadiene moiety flanked by two polycyclic aromatic rings] but by a molecular arrangement of the two naphthyls which could allow a different adaptability to the DNA interstrand cavity.

Herein we analyze the antiproliferative activity of 2-Naph-DNB together with its ability to trigger apoptosis, to up-regulate p53 protein, to cause modifications of the cell cycle and to bind to DNA forming ISCL. Moreover, data about the lethal and toxic effects *in vivo* of 2-Naph-DNB have also been obtained.

2. Materials and methods

2.1. Chemistry

Likewise 1-Naph-DNB, 2-Naph-DNB is a stable, fully characterized diaryldinitrobutadiene deriving from the initial ring-opening of 3,4-dinitrothiophene [14–17]. The synthesis of 2-Naph-DNB has been achieved via arylation of 1,4-bis(diethylamino)-2,3-dinitro-1,3-butadiene with 2-naphthylmagnesium bromide (see Scheme 1) as described hereinafter.

A solution of (1*E*,3*E*)-1,4-bis(diethylamino)-2,3-dinitro-1,3-butadiene (1 mmol, 300 mg; synthesized from 3,4-dinitrothiophene as previously reported in Ref. [14]) in tetrahydrofuran (THF, 10 ml) was cooled to 0 °C under magnetic stirring. The calculated amount of a ca. 0.5 M solution of 2-naphthylmagnesium bromide (2.2 mmol) in THF was slowly added by syringe and the reaction mixture left under stirring at the same temperature until disappearance of the substrate (ca. 1 h), the progress of the reaction being monitored by TLC. Quenching of the reaction was performed by pouring the final solution, with vigorous shaking, into a mixture of dichloromethane/ice water containing 2.2 mmol of HCl. After extraction with dichloromethane, the organic phase was washed with water, dried with Na_2SO_4 and rotoevaporated to dryness. The product (98% yield) is obtained in quite pure form by chromatography of the residue on a silica gel (63–200 mesh) column eluted with a gradient of dichloromethane and petroleum ether. 2-Naph-DNB is a yellow solid, mp 179–180 °C (light petroleum/toluene); ^{1}H NMR ($CDCl_3$) δ 7.41–7.56 (6H, m), 7.68–7.75 (6H, m), 7.90 (2H, s), 8.71 (2H, s); ^{13}C NMR ($CDCl_3$) δ 124.5, 127.1, 127.2, 127.8, 128.9, 129.0, 129.4, 132.8, 133.8, 134.7, 140.1, 141.6. ESI (Electrospray Ionization)-MS: *m/z* 418.9 ($M + Na^+$), 815.1 ($2M + Na^+$).

^{1}H NMR and ^{13}C NMR spectra were recorded on a Varian Mercury 300 spectrometer at 300 MHz and 60 MHz, respectively (TMS as internal reference). The ESI-MS spectrum was acquired on a ZMD Micromass single quadrupole mass spectrometer operating at 4000 *m/z*. The melting point was determined with a Büchi 535 apparatus and is uncorrected. Petroleum ether and light petroleum refer to the fractions with bp 40–60 °C and 80–110 °C, respectively. THF was purified by standard methods and distilled over potassium benzophenone ketyl before

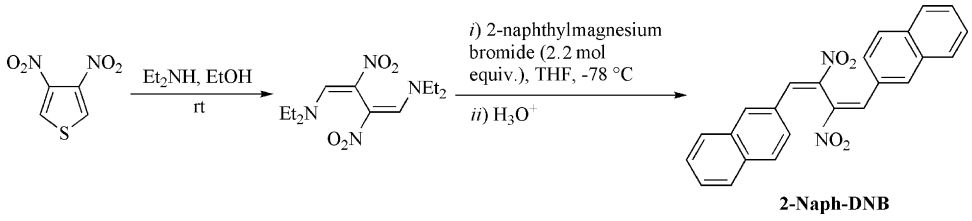

Scheme 1.

use. All other commercially available reagents were used as received.

2.2. In vitro

2.2.1. Growth inhibition assay

Nine human and murine cell lines (human: A2780, (ovary, carcinoma) [18], A549 (lung, carcinoma) [19], H1299 (lung, carcinoma, kindly provided by Dr. K. Okaichi) [20], HGC-27 (stomach, carcinoma) [21], HCT-8 (colon, adenocarcinoma) [22], Jurkat (T cell leukaemia) [23], MDA-MB-231 (breast, adenocarcinoma) [24], PA-1 (ovary, teratocarcinoma) [25]; murine: P388 (leukaemia) [26]) were plated into 96-well microtiter plates at different concentrations/well (range: 1500–5000/well) for about 8 h. 2-Naph-DNB was added in duplicate at the appropriate concentrations for a minimum of five concentrations (two to three-fold serial dilutions). A final volume of 200 μl was reached in each well. After 3-day culture 50 μl of 3-(2,5-dimethyl-2-thiazolyl)-2,5-diphenyl-2H-tetrazolium bromide (MTT, Sigma, St. Louis, MO, USA) solution [2 mg/ml in phosphate buffered saline (PBS)] was added to the wells and incubated for 4 h at 37 °C. Microplates were then centrifuged at 275 g for 5 min and the culture medium carefully aspirated and replaced with 100 μl of 100% dimethylsulfoxide. Complete and homogeneous solubilization of formazan crystals was achieved after 20 min of incubation and shaking of well contents. The absorbance was measured on a 400 ATC microculture plate reader (SLT Labinstruments, Austria) at 540 nm [27]. IC_{50}'s were calculated by the analysis of single-dose response curves, each final value being the mean of 4–11 independent experiments.

2.2.2. Trypan blue (TB) dye exclusion assay and visualization of apoptotic cells/nuclei by 4′-6-diamidino-2-phenylindole (DAPI) staining

Cell lines were plated at different cell concentrations/well (range: 10,000–30,000/well) into 24-well microtiter plates for about 8 h, then 2-Naph-DNB was administered at its specific IC_{50} and IC_{75}, as calculated with the MTT assay. After 72 h cells were harvested, washed twice with cold PBS and splitted in two halves. One half of cells was concentrated to 100 μl normal saline and stained with 5 μl of TB (0.4% in 0.81% sodium chloride and 0.06% potassium phosphate dibasic). The percentage of stained dead cells was evaluated at the microscope.

The other half was fixed with 100 μl of 70% ethanol in PBS and maintained at 4 °C. For the examination at the microscope, 5 μl of a solution of 10 μg/ml DAPI in water was added and immediately after the percentage of apoptotic segmented nuclei/cells was evaluated.

2.2.3. Western blot analysis of p53

Human A2780, A549, Jurkat, MDA-MD-231, PA-1 and HGC-27 cells were treated with their specific IC_{50}s of 2-Naph-DNB, as previously evaluated by the MTT assay. After 24 and 48 h culture control and treated cells were harvested, washed twice with cold PBS and treated with a lysis buffer [1% Triton X-100, 0.15 M NaCl and 10 mM Tris (pH 7.4)] containing protease inhibitors (50 mg/ml phenylmethylsulphonyl fluoride and 2 mg/ml aprotinin) for 30 min at 4 °C. The protein concentration was determined by the Bradford method (Sigma Chemical Co., St. Louis, MO, USA). Equal amounts of total protein (30–60 μg) were separated on a 12% polyacrylamide gel (SDS-PAGE). Proteins were transferred onto a nitrocellulose membrane (Hybond C-Extra, Amersham Italia Srl, Milan, Italy) and protein loading checked by Ponceau S staining. Nonspecific binding was blocked overnight at 4 °C with 1% bovine albumin (Sigma) in Tris–buffered saline–Tween 20 [0.15 M NaCl, 10 mM Tris (pH 8.0), 0.05% Tween 20]. Blots were probed with anti-p53 DO-1 (1:2000, Santa Cruz, CA, USA) monoclonal antibodies. After incubation with horseradish peroxidase-conjugated antimouse IgG, bands were visualized by chemiluminescent detection (ECL™ Western blotting analysis system, Amersham Italia Srl) following the supplier's recommended procedures. Prestained molecular weight markers (New England Biolabs, Beverly, MA, USA) were used as reference.

Alternatively, A549 cells were incubated for 72 h with different concentrations of 2-Naph-DNB. Cells were then treated and p53 analyzed as described before.

Densitometric normalization was performed by using the expression signal obtained by an anti-α/β-tubulin monoclonal antibody (TU-10,1:5000, Santa Cruz, CA, USA).

2.2.4. Analysis of the cell cycle

A549, Jurkat and HGC-27 cells were also analysed for the effect of 2-Naph-DNB on cell cycle phases. Cells ($1–2 \times 10^6$) were treated for 48 h with three different concentrations of our molecule, harvested, washed twice with cold PBS and fixed in 70% ethyl alcohol at −20 °C overnight. After fixation, cells were centrifuged, washed with PBS, and incubated at room temperature for 20 min with propidium iodide (PI) staining solution (50 μg/ml PI, 0.05% Triton X-100, 20 mg/ml RNase A in PBS). Cells were analyzed by flow cytometric analysis of DNA content using FACSort flow cytometer (BD Biosciences, Mountain View, CA). The percentages of cell cycle distribution were calculated by ModFit LT computer program.

2.2.5. Analysis of interstrand cross-link (ISCL)

The % ISCL was evaluated using, as target, pure DNA extracted from P388 cells by the salting out technique [28] (260/280 = 1.84) and dissolved in distilled water. Two different concentrations (1.0 and 0.1 μM) of 2-Naph-DNB were incubated with DNA (final concentration: 485 μg/ml) for 1 h at 37 °C, then DNA was precipitated with sodium acetate and ethanol and resuspended in Tris–buffered saline–Tween 20. A solution (1.5 ml) of ethidium bromide (10 μg/ml in 0.4 mM EDTA, 20 mM K_2HPO_4, pH 11.8) was added to 0.2 ml (10 μg) aliquots of DNA extracted from control and treated cells. The fluorescence was measured before and after heating at 95 °C for 8 min (Fluoroskan Ascent, Thermolab Systems; excitation wavelength, 530 nm; emission wavelength, 590 nm) in 96 microtiter plates, while the final volume in the wells was 300 μl. The % ISCL was determined according to the formula $(ft - fn)/(1 - fn) \times 100$, where ft and fn were the fluorescence

after denaturation divided by the fluorescence before denaturation of treated (ft) and control (fn) samples.

2.3. In vivo

2.3.1. Animals

Female CD1 mice (20–25 g, Harlan Italy, S. Pietro al Natisone, Italy) were allowed a 7-day period before use. Standard food and water ad libitum were available at all time. All experiments were performed in accordance with the guidelines of the Federation of European Laboratory Animal Science Associations and approved by the Institutional Review Board for animal studies.

2.3.2. Toxicological testing

The determination of lethal and maximal tolerated doses was performed in normal female CD1 mice by daily observation of toxicity sign and survival. Groups of 8 + 2 satellite animals were treated i.v. with a single injection of 2.5, 5, 7.5, 10 and 15 mg kg^{-1} of 2-Naph-DNB. LD_{10}, LD_{50} and LD_{90} parameters were calculated using deaths up to 14 days after administration. By the same experiments we also evaluated the MTD, as the maximal administered dose of Naph-DNB without significant toxic effects.

2-Naph-DNB was diluted in DMSO and given in a volume not exceeding 1 μl g^{-1} of body weight in order to avoid toxic effects of the solvent. Body weight was recorded every 2 days.

Satellite animals were sacrificed with CO_2 on day 4 or when dying. Immediately after autopsy fresh tissues obtained from organ explants were fixed and processed for histological analysis.

2.3.3. Light microscopy

For light-microscopy studies, fragments of liver, kidney, spleen, lung and heart were fixed for 24 h in 2% paraformaldehyde in 0.1 M PBS, pH 7.4, processed routinely, embedded in Paraplast wax, and sectioned at 6 μm.

Sample sections of all the tissues were stained with hematoxylin and eosin (H&E). Moreover, the Perls' Prussian Blue reaction was performed on samples from liver and spleen, to detect ferric pigments content. Liver sections underwent PAS staining (with and without α-amylase digestion) to detect glycogen; PAS reaction was performed also on kidney sections. All the samples were evaluated qualitatively.

2.4. Statistical analysis

The Mann–Whitney and Friedman ANOVA & Kendall's Concordance tests for not parametric data and the unpaired Student's *t* test were used for statistical analysis of data.

3. Results

3.1. In vitro

3.1.1. Antiproliferative activity and induction of apoptosis

The IC_{50} values obtained from the concentration–response curves designed after the treatment of the different cell lines with 2-Naph-DNB showed that this molecule is characterized by a good antiproliferative activity, with IC_{50}s and IC_{75}s ranging in the 1.7 ± 0.4–13.4 ± 3.4 μM range of concentrations (Median IC_{50} = 4.7 μM) and 3.4 ± 0.1–22.5 ± 6.7 μM (Median IC_{75} = 10.1 μM), respectively (Table 1). The cell lines most sensitive to the exposure to 2-Naph-DNB were P388, A2780 and PA-1. A good antiproliferative activity was also recorded against the p53-null human H1299 lung carcinoma cell line (Table 1).

Table 1
In vitro determination of inhibition of cell proliferation (MTT) by 2-Naph-DNB

Cell line	Histotype/origin	2-Naph-DNB	
		IC_{50}	IC_{75}
P388	Leukemia/mouse	1.7 ± 0.4[a]	3.4 ± 0.1
A2780	Ovary/human	3.9 ± 1.0	5.9 ± 1.5
PA-1	Ovary/human	2.9 ± 0.8	4.6 ± 0.9
Jurkat	Leukemia/human	5.1 ± 1.2	11.7 ± 2.1
HGC-27	Stomach/human	4.7 ± 0.8	7.2 ± 1.6
MDA-MB-231	Breast/human	5.9 ± 1.6	12.3 ± 2.9
HCT-8	Colon/human	13.9 ± 1.6	19.8 ± 4.4
A549	Lung/human	13.4 ± 3.4	22.5 ± 6.7
H1299	Lung/human	3.6 ± 0.8	10.1 ± 2.2

[a] Data express the mean ± S.D. of 4–11 experiments.

A similar result was obtained considering the cytotoxic activity, as determined by the trypan blue dye exclusion assay, and exposing cells to their specific IC_{50} (Median % TB^+ cells = 20%) and IC_{75} (Median % TB^+ cells = 40%), as determined by the MTT assay. Also in this case P388, A2780, and Jurkat proved to be most sensitive to the cytotoxic activity of 2-Naph-DNB. Interestingly, also H1299 showed a discrete sensitivity to the cytotoxic activity of our nitrobutadiene compound (Fig. 2).

Finally, we analyzed the induction of apoptosis by the observation of nuclear segmentation after DAPI staining. Although only Jurkat cells showed a high sensitivity when exposed to the

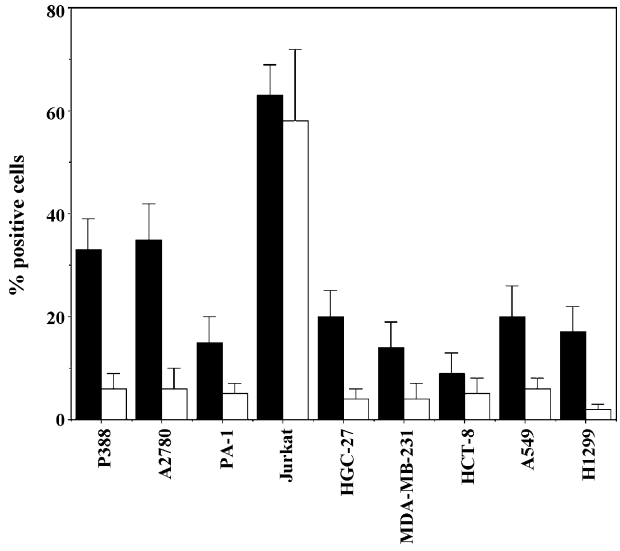

Fig. 2. Histograms represent the percentage of cells stained with the TB (■, dead cells) or DAPI (□, apoptotic cells) dyes after 72 h exposure to the corresponding IC_{50}s of 2-Naph-DNB.

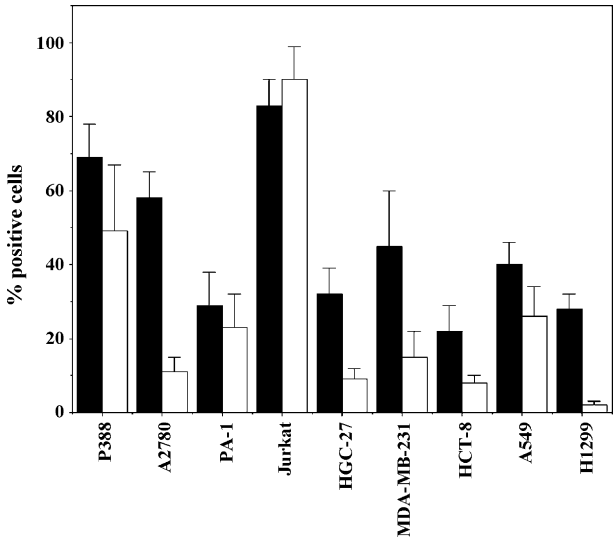

Fig. 3. Histograms represent the percentage of cells stained with the TB (■, dead cells) or DAPI (□, apoptotic cells) dyes after 72 h exposure to the corresponding IC_{75}s of 2-Naph-DNB.

IC_{50} of 2-Naph-DNB (as evaluated by the MTT assay), when we applied the IC_{75} the percentage of apoptotic cells increased significantly, particularly in P388, PA-1, Jurkat, and A549 cells (range: 23–90%) (Fig. 3). As expected, no apoptotic cells were recorded when p53-null H1299 cells were treated with both concentrations.

3.1.2. Western blot analysis

Analysis by western blot of p53 oncoprotein was performed in A549, A2780, PA-1, MDA-MB-231 and Jurkat cells. In all cell lines 2-Naph-DNB was able to up-regulate p53 with relative maximal increases of p53 concentration ranging from +5% to +245%. In terms of protein increase, cells with wild type p53 (A2780, A549 and PA-1) seem to have an oncoprotein upregulation higher than that observed in MDA-MB-231 provided of a mutated form of p53.

Maximal protein increase (Fig. 4A) was reached at different times for different cell lines and, in spite of the limited number of time points used for this determination, our data reveal different kinetics for the upregulation of p53. Moreover, upregulation was clearly concentration-dependent, as demonstrated in A549 cells after 72 h exposure (Fig. 4B).

3.1.3. Cell cycle

A549, Jurkat and HGC-27 cells were also analyzed for the modifications of cell-cycle phase after exposure to increasing concentrations of 2-Naph-DNB. As shown in Table 2, our data display that 2-Naph-DNB was able to significantly cause a partial block of cells in the G2/M phase of the cell cycle, with a concomitant decrease of cells in the S phase. While in HGC-27 cells this effect showed a clear trend toward a correlation with the applied concentrations of 2-Naph-DNB ($p < 0.07$), in A549 and Jurkat cells it becomes significant versus control cells only at the higher concentrations ($p < 0.05$) (Table 2).

3.1.4. Interstrand cross-links

2-Naph-DNB was tested for its ability to form ISCL. In a free-cell system using pure DNA isolated from P388 cells as target, our compound was able to form ISCL, although the % ISCL recorded was lower than expected (Fig. 5) if compared to the results obtained with 1-Naph-DNB [10]. Moreover, it is noteworthy that when the % ISCL was evaluated on DNA extracted from A549, A2780 and Jurkat cells treated with 2-Naph-DNB for 6 h at their IC_{50} (as calculated by the MTT assay)

Table 2
Percentage of A549, Jurkat, and HGC-27 cells in the different cell-cycle phases after treatment with different concentrations of 2-Naph-DNB

Cell line	Cell-cycle phase	Concentration of 2-Naph-DNB (μM)			
		0	6.25	25	100
A549	G0/G1	40.7 ± 6.5[a]	37.7 ± 3.9	50.6 ± 5.8	34.5 ± 0.3
	S	37.1 ± 0.8	38.7 ± 1.2	29.2 ± 5.1	20.3 ± 1.5[b]
	G2/M	22.2 ± 6.5	23.6 ± 4.6	20.2 ± 0.4	45.3 ± 1.8[b]
Cell line	Cell-cycle phase	Concentration of 2-Naph-DNB (μM)			
		0	0.94	3.75	15
Jurkat	G0/G1	41.6 ± 4.8	40.6 ± 5.5	35.3 ± 1.5	46.3 ± 3.4
	S	36.1 ± 4.7	37.1 ± 6.4	41.3 ± 2.4	23.1 ± 4.7[b]
	G2/M	22.3 ± 2.1	22.3 ± 2.3	23.4 ± 2.8	30.6 ± 6.6[b]
Cell line	Cell-cycle phase	Concentration of 2-Naph-DNB (μM)			
		0	1.88	7.5	30
HGC-27	G0/G1	37.1 ± 0.9	33.8 ± 4.3	36.2 ± 1.8	46.8 ± 1.2
	S	38.1 ± 0.8	35.2 ± 5.5	30.6 ± 2.8[b]	23.8 ± 2.9[b]
	G2/M	24.8 ± 0.5	31.2 ± 1.6[b]	33.2 ± 1.7[b]	29.4 ± 2.5[b]

[a] Mean ± S.D. of 3/4 data.
[b] $p < 0.05$, as determined by the Mann–Whitney-test for not parametric data.

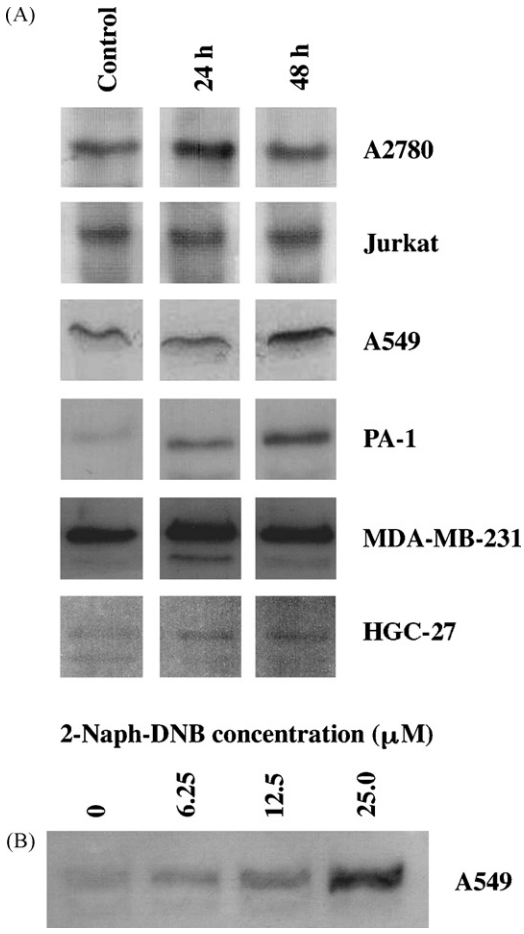

Fig. 4. (A) Western blot analysis of p53 after exposure of different cell lines to the corresponding IC_{50}s of 2-Naph-DNB, calculated by the MTT assay. Prestained molecular markers were always included as references. Control was harvested after 48 h. (B) Representative Western blot analysis of p53 after exposure of A549 cells to increasing concentrations of 2-Naph-DNB.

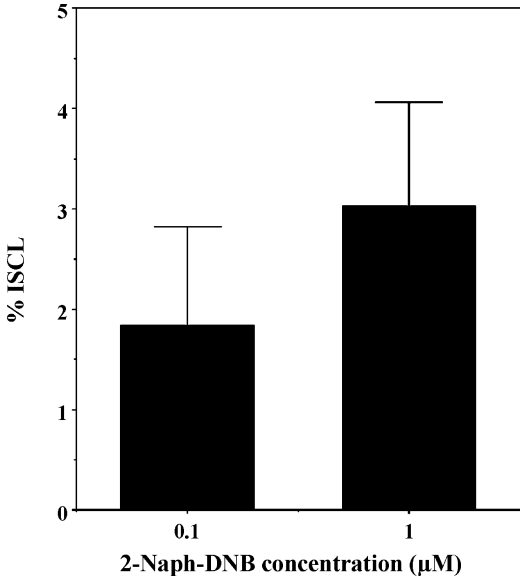

Fig. 5. Histograms represent the % ISCL obtained exposing pure DNA extracted from murine P388 cells to different concentrations of 2-Naph-DNB for 1 h. Histograms represent the mean ± S.D. of three data.

the % ISCL recorded was again lower than that observed for the parent compound 1-Naph-DNB (in general < 1%, data not shown).

3.2. In vivo

3.2.1. Toxicity studies

Based on the percentage of died CD1 mice treated with single administration of 2-Naph-DNB i.v., we determined the LD and MTD shown in Table 3. By the same experiments we also calculated both the MTD and the percent variation of body weight (Table 3).

Extravasation of 2-Naph-DNB caused a reversible caudal ulcer and, as in the case of 1-Naph-DNB [12], it was not completely healed 14 days after administration (not shown).

3.2.2. Morphology and histochemistry

From a morphological point of view all the organs of the control animals showed a normal structural aspect (data not shown).

Histochemical analysis of control liver revealed typical glycogen zonation within the parenchyma submitted to PAS reaction. In particular, cells surrounding pericentral vein were more intensely stained compared to periportal cells. In the same sections, very light Perls' reactivity was generally observed in the hepatocytes and endothelial cells.

The liver parenchyma of samples treated with low doses of 2-Naph-DNB (2.5 and 5 mg kg^{-1}) was structurally similar to controls (Fig. 6A). PAS positivity was still mainly concentrated in pericentral hepatocytes, though a slight decrease in intensity was observed after treatment with 5 mg kg^{-1} of 2-Naph-DNB (Fig. 6B). After Perls' method a light cytoplasmic staining occurred in hepatocytes. More intense reactivity was seen in sinusoidal cells (Fig. 6C).

Severe changes were noted in parenchyma of mice treated with the highest doses of 2-Naph-DNB (7.5 and 10 mg kg^{-1}). A process of hepatocytic alteration affected the parenchyma irregularly, mainly at 10 mg kg^{-1}. Most cells displayed light cytoplasm and several nuclei were apoptotic. Moreover, sinusoids and some

Table 3
Determination of lethal doses (LD) and maximal tolerated dose (MTD) in CD1 mice treated with single doses i.v. of 2-Naph-DNB (upper table) and percent weight loss on days +2 and +4

Route of administration	LD_{10}	LD_{50}	LD_{90}	MTD
i.v.	3.5[a]	6.8	11.9	2.8

Day of observation	Doses of 2-Naph-DNB (mg kg^{-1})				
	2.5	5	7.5	10	20
+2	−1.8	−0.1	−3.9	−11.5	–[b]
+4	+1.7	+3.3	−2.7	–[c]	–

[a] Values represent the doses expressed in mg kg^{-1}. Animals were treated and then observed for 14 days.
[b] All animals died by day +2.
[c] All animals but two died by day +4.

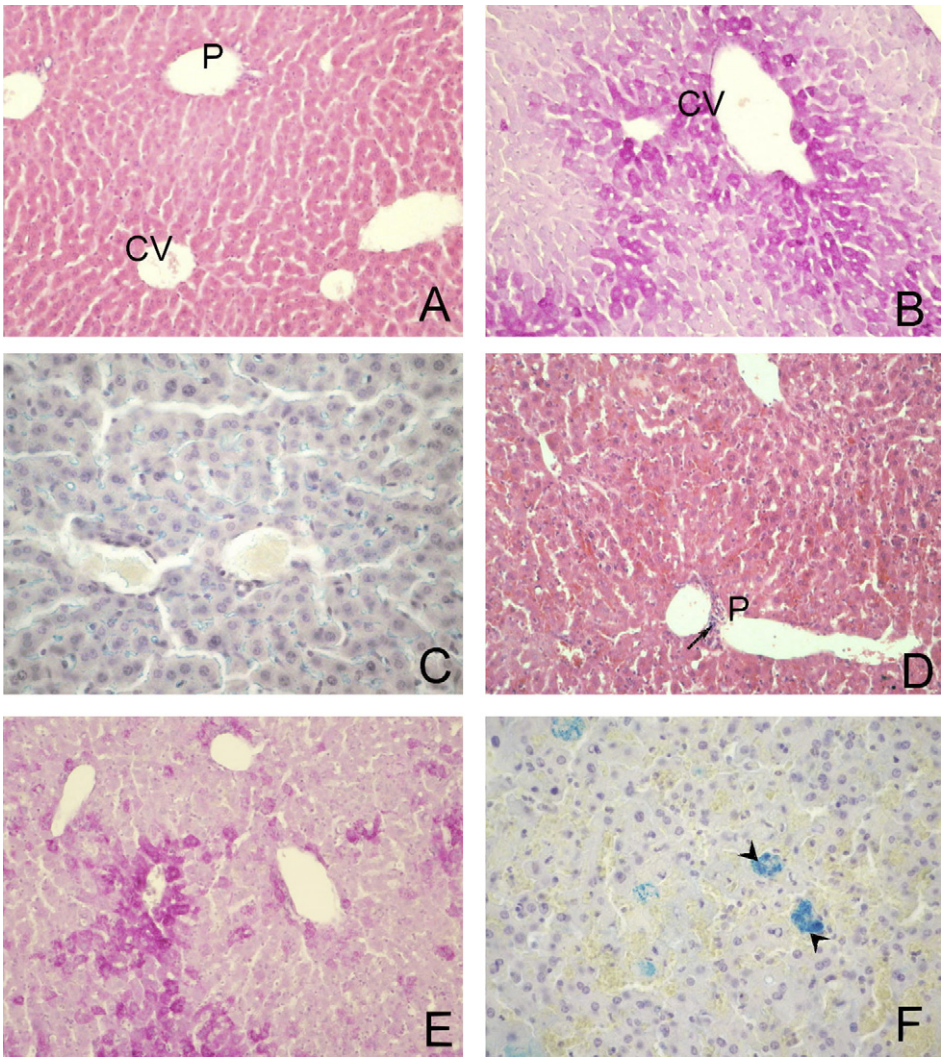

Fig. 6. Liver from representative treated mice with 5 mg kg^{-1} (A–C) and 10 mg kg^{-1} 2-Naph-DNB (D–F); sections stained with H&E (A and D), PAS reaction (B and E) and Perls' technique (C and F). At low dose the hepatocytes surrounding both portal tract (P) and central vein (CV) show no pathological changes; moderate/intense perivenous PAS staining is noted in most hepatocytes. In (C), Perls' staining is evident in the endothelial cells. Sections from mice treated with 10 mg kg^{-1} 2-Naph-DNB show altered hepatocytes, sinusoids filled with red cells and leucocytes infiltration in the portal (P) space (arrow). PAS staining is irregularly observed in the parenchyma. In (F), note large hepatocytes that show intense blue iron staining (arrowheads). A, B, D and E, 100×; C and F, 200×.

vessels appeared greatly congested with erythrocytes, and a mild infiltration of leukocytes was sometimes observed in portal areas (Fig. 6D). PAS staining displayed an irregular distribution of glycogen content around the central vein, caused by the presence of hepatocytes with high staining intensity among most hepatocytes with considerably lower positivity (Fig. 6E). In general, light to moderate Pearls' reactivity was observed in the parenchyma, except for occasional large hepatocytes that contained abundant blue deposits (Fig. 6F).

The spleen parenchyma of both control animals and those treated with low doses of 2-Naph-DNB showed distinct areas of white and red pulp (Fig. 7A). The red pulp was characterized by moderate to intense Perls' reactivity, mainly in the cells of the reticulo-endothelial system. Light positivity was also observed along blood capillaries in the white pulp (Fig. 7B). However, starting from the dose of 5 mg kg^{-1} numerous megakaryocytes were observed within the red pulp (Fig. 7C). At the highest doses spleens exhibited partial disruption of follicular architecture and the red pulp displayed a remarkable congestion of erythrocytes (Fig. 7D). In the same samples the Perls' staining was diminished (Fig. 7E). Moreover, in the white pulp the capillaries appeared dilated and contained leucocytes (Fig. 7F).

The morphology of the kidney parenchyma of samples treated with the lowest dose of 2-Naph-DNB was similar to control (Fig. 8A,B). Starting from the dose of 5 mg kg^{-1} occasional proximal tubules displayed epithelia cells with light cytoplasm and irregular brush border. At the highest doses of 2-Naph-DNB (7.5 and 10 mg kg^{-1}) more tubules appeared altered, and most capillaries intermingled with tubules were dilated (Fig. 8C). In particular, the PAS reaction evidenced irregular profiles of the epithelia constituting the proximal tubules (Fig. 8D).

4. Discussion

Our recent data [10–13] both *in vitro* and *in vivo* have shown that 1-Naph-DNB possesses a significant antitumour activity

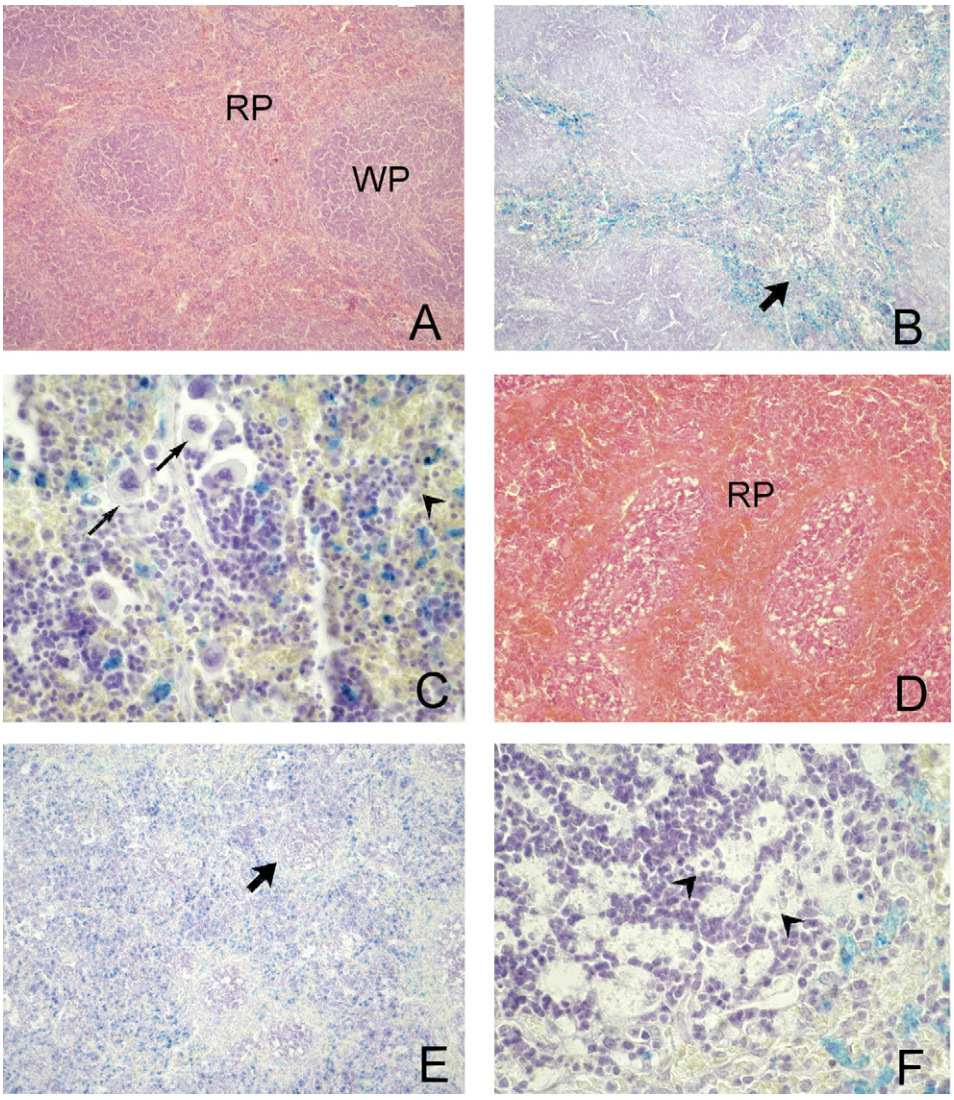

Fig. 7. Spleen from representative treated mice with 5 mg kg^{-1} (A and B), 7.5 (C) and 10 mg kg^{-1} 2-Naph-DNB (E and F); sections stained with H&E (A and D), and Perls' technique (B, C, E and F). Characteristic morphology of the spleen parenchyma is noted in samples treated with low dose; the white pulp (WP) shows a definite structural organization and is surrounded by the red pulp (RP) (A). Very intense Perls' staining is observed in the red pulp (B, thick arrow). After the treatment with 7.5 mg kg^{-1} 2-Naph-DNB note the presence of megakaryocytes in the red pulp (C, arrows). With the highest dose, the RP appears congested with erythrocytes (D). While the red pulp shows a reduced Perls' reactivity, it is to note the irregular organisation of the white pulp (E, thick arrow). Note dilated capillaries in the white pulp (F, arrowheads). A, B, D and E, 100×; C and F, 600×.

mainly based on its binding to DNA and on the following activation of the apoptotic machinery.

In the perspective of using 1-Naph-DNB as a lead compound, purposely devised functional modifications have revealed [unpublished data] that the pharmacological activity of such molecules essentially rests on the 1-naphthyl-2-nitro-1,3-butadiene array. In this line, 2-Naph-DNB has been devised as a purely structural (rather than functional) modification of the lead, possibly able to determine a better adaptability of the molecule within the tumour-cell DNA double strand, thus enforcing, in particular, a pharmacologically more significant antiproliferative activity. Such an outcome would definitely provide new anticancer compounds to be confidently subjected to *in vivo* experiments.

As a matter of fact, our outcomes show that 2-Naph-DNB is definitely less capable than 1-Naph-DNB to form ISCL when tested in a cell-free system on pure DNA or when tested directly on cells. Nonetheless, in spite of its lower ability to form ISCL, 2-Naph-DNB possesses a good antiproliferative activity (although different in terms of specificity if compared to 1-Naph-DNB: see below in the discussion) also when this activity is evaluated in terms of cytotoxicity and/or induction of apoptosis. In particular, the *in vitro* behaviour of 2-Naph-DNB interestingly suggests that this compound is able to ensure a good antiproliferative activity against various tumour cells of different histological origin. Fig. 9 illustrates, in terms of IC_{50} for the MTT assay, the relative change in specificity of 2-Naph-DNB compared to 1-Naph-DNB: thus, while more pharmacologically significant effects of the 2-naphthyl derivative were found in HGC-27 and MDA-MB-231 cells, the prevalent antiproliferative activity in A2780, Jurkat and HCT-8 cells was due to 1-Naph-DNB.

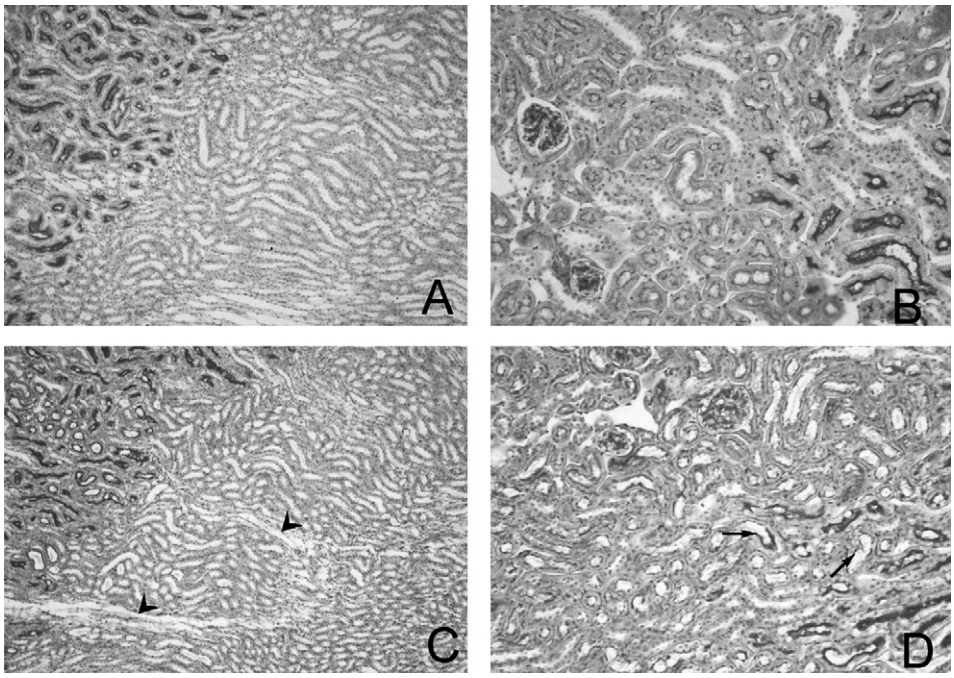

Fig. 8. Kidney from representative treated mice with 2.5 mg kg^{-1} (A and B) and with 10 mg kg^{-1} (C and D) 2-Naph-DNB; sections stained with PAS reaction. After the low dose treatment the parenchyma shows normal morphology. With high dosage peritubular vessels appear dilated (arrowheads); numerous tubules, and especially proximal tubules display irregular luminal profiles (arrows). A and B, 100×; B and D, 200×.

Therefore our data, while not excluding a possible interaction with the tumour-cell DNA, on the other hand open the possibility of a mechanism of action different from that hypothesized for 1-Naph-DNB. Such a result could be also supported by our unpublished data from our laboratory about the cross-resistance in taxol-resistant cells, made resistant *in vitro* by means of the induction of a point mutation of α-tubulin able to alter the stability of microtubules. This in turn suggests the possibility of previously unveiled mechanisms of action for 2-Naph-DNB.

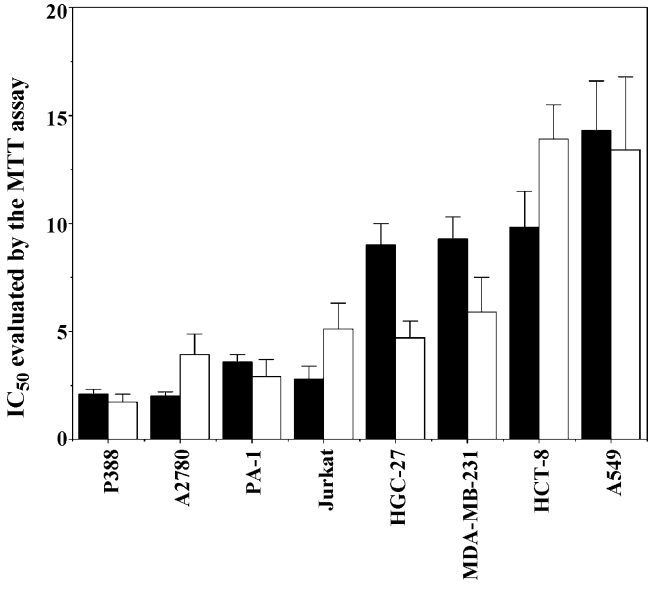

Fig. 9. Comparison between the IC_{50}s calculated by the MTT assay after 72 h exposure to 1-Naph-DNB (■) and 2-Naph-DNB (□). *p*-values: P388, $p < 0.05$; A2780, $p < 0.01$; PA-1, NS; Jurkat, $p < 0.01$; HGC-27, $p < 0.001$; MDA-MB-231, $p < 0.01$; HCT-8, $p < 0.001$; A549, NS.

Although some doubts may still remain about the effective role of apoptosis in clinical setting, the hypothesis that this physiological pathway of cell death may be of relevance to the response to anticancer drugs in human patients is generally accepted [29–34]. This is the reason why one property that compounds with antiproliferative properties must have, in order to be considered deserving of a possible development as anticancer drugs, is the ability to trigger apoptosis. This feature has actually been confirmed herein, 2-Naph-DNB being able to activate p53 (in a concentration-dependent manner and with a different timing of upregulation in different cells) and to induce nuclear segmentation, the typical nuclear morphology of apoptotic cells. 2-Naph-DNB seems also definitely able to up-regulate p53 better in cells with a wild type form than in cells endowed with a mutated form, although the low number of cell lines involved in this study may not allow final conclusions about this point. The activation of p53 could confirm the binding of 2-Naph-DNB to DNA and its damage in spite of the reduced formation of ISCL recorded by our experiments.

On the other hand, our finding that the percentage of cells in apoptosis (as evaluated by DAPI staining) was about nine times (2% versus 17.5% at the IC_{50}) lower than the percentage of cells stained by the TB dye in p53-null H1299 cells suggests that the oncosuppressor gene p53 is critical for the activation of the apoptotic machinery by 2-Naph-DNB. Moreover, the fact that also at high concentration (IC_{75}) we did not observe apoptotic cells (Fig. 3) strengthens this conclusion.

Furthermore, the ability of our nitrobutadiene compound to block cells in the G2/M phase of the cell cycle in a concentration-dependent manner represents a rather strong hint for an effective

link between DNA (or other targets to be identified) damage, p53 activation, block in G2/M phase of the cell cycle and apoptosis.

Altogether, the data collected seem to nicely fulfil our expectations, suggesting that a purely structural (rather than functional) modification of the 1-Naph-DNB lead, devised with the hope to increase the link or intercalation of 2-Naph-DNB to DNA, may significantly influence the antiproliferative activity of the original molecule, in particular against HGC-27 and MDA-MB-231 cells, i.e. those derived from tumour histotypes less responsive to chemotherapeutics.

Our *in vivo* toxicity experiments allowed both the definition of LDs and of MTD parameters useful for the following evaluation *in vivo* and the analysis of tissue damage due to treatment with increasing doses of 2-Naph-DNB. On the basis of histochemical analysis prominent changes have regarded liver and spleen, although depending on the dosage used. At the highest doses, the presence of congested vessels in both the organs suggests a possible mechanism of toxicity due to a progressive ischemic injury. However, in the liver we cannot exclude a primary interaction of the molecule with the hepatocytes, as evidenced by the altered PAS positivity, the elevated Perls' reactivity of some hepatocytes, and the presence of apoptotic cells. On the other hand, the prominent involvement of this organ in the detoxifying processes makes hepatocytes sensitive to drugs mainly if administered at high dosage.

Changes in haemopoietic/haemocatheretic engagement of spleen, mainly observed in high-dose treated mice, are probably related to changes of the vascular conditions in both liver and spleen. In particular, while the distribution of the Perls' reaction in spleen of control and low-dose treated samples is in keeping with the normal distribution of ferritin and hemosiderin in this normally hemocatheretic organ, the decreased reactivity observed in high-dose treated samples and the concomitant presence of numerous megakaryocytes, suggest an increase of hemopoiesis. This fact, also evidenced after the treatment with 1-Naph-DNB (Invest New Drug, in press) probably reflects an impairment of the bone marrow due to the treatment.

Similarly to 1-Naph-DNB, the isomer herein seems to produce less consistent damages in the kidney, where some alterations of both tubules and vessels appeared at the highest doses.

In conclusion, our data demonstrate that the new molecule 2-Naph-DNB, an isomer originated by a modification of the structure of the lead compound 1-Naph-DNB which essentially influences the molecular geometry, possesses appreciable antiproliferative, cytotoxic and pro-apoptotic activities together with a low profile of toxicity *in vivo*. Although our effort, as expected, did not solve the problem of the low solubility of the lead compound 1-Naph-DNB, they definitely demonstrate the possibility to increase the activity or modify the specificity of our nitrobutadiene compounds by simply modifying their geometrical array.

Acknowledgments

This research was supported by funds from M.I.U.R. (FIRB 2001) and from the Universities of Genova and Bologna. C. Prevosto is recipient of a fellowship awarded by the Italian Foundation for Cancer Research (FIRC).

References

[1] Ferlay J, Bray F, Pisani P, Parkin DM. Globocan 2000: cancer incidence, mortality and prevalence worldwide, version 1.0 (IARC, CancerBase No 5). Lyon: IARC Press; 2001.
[2] Parkin DM, Bray F, Ferlay J, Pisani P. Global cancer statistics, 2002. CA Cancer J Clin 2005;55:74–108.
[3] Kamangar F, Dores GM, Anderson WF. Patterns of cancer incidence, mortality, and prevalence across five continents: defining priorities to reduce cancer disparities in different geographic regions of the world. J Clin Oncol 2006;24:2137–50.
[4] Omenn GS, Goodman GE, Thornquist MD, Balmes J, Cullen MR, Glass A, et al. Effects of a combination of beta carotene and vitamin A on lung cancer and cardiovascular disease. N Engl J Med 1996;334:1150–5.
[5] Luqmani YA. Mechanisms of drug resistance in cancer chemotherapy. Med Princ Pract 2005;14(Suppl. 1):35–48.
[6] Donnenberg VS, Donnenberg AD. Multiple drug resistance in cancer revisited: the cancer stem cell hypothesis. J Clin Pharmacol 2005;45: 872–7.
[7] Longley DB, Johnston PG. Molecular mechanisms of drug resistance. J Pathol 2005;205:275–92.
[8] Schwartsmann G, Ratain MJ, Cragg GM, Wong JE, Saijo N, Parkinson DR, et al. Anticancer drug discovery and development throughout the world. J Clin Oncol 2002;20(Suppl. 15):47S–59S.
[9] Neidle S, Thurston DE. Chemical approaches to the discovery and development of cancer therapies. Nat Rev Cancer 2005;5:285–96.
[10] Viale M, Ottone M, Chiavarina B, Mariggiò MA, Prevosto C, Dell'Erba C, et al. Preliminary evaluation in vitro of the inhibition of cell proliferation, cytotoxicity and induction of apoptosis by 1,4-bis(1-naphthyl)-2,3-dinitro-1,3-butadiene. Invest New Drug 2004;22:359–67.
[11] Novi M, Ottone M, Dell'Erba C, Barbieri F, Chiavarina B, Maccagno M, et al. 1,4-Bis(1-naphthyl)-2,3-dinitro-1,3-butadiene a novel anticancer compound effective against tumour cell lines characterized by different mechanisms of resistance. Oncol Rep 2004;12:91–6.
[12] Dell'Erba C, Chiavarina B, Fenoglio C, Petrillo G, Cordazzo C, Boncompagni E, et al. Inhibition of cell proliferation, cytotoxicity and induction of apoptosis of 1,4-bis(1-naphthyl)-2,3-dinitro-1,3-butadiene in gastrointestinal tumour cell lines and preliminary evaluation of its toxicity in vivo. Pharmacol Res 2005;52:271–82.
[13] Petrillo G, Fenoglio C, Ognio E, Aiello C, Spinelli D, Mariggiò MA, Maccagno M, Morganti S, Cordazzo C, Viale M. Naphthylnitrobutadienes as pharmacologically-active molecules: evaluation of the in vivo antitumour activity. Invest New Drug 2007; doi:10.1007/s10637-007-9065-4.
[14] Dell'Erba C, Mele A, Novi M, Petrillo G, Stagnaro P. Synthetic exploitation of the ring-opening of 3,4-dinitrothiophene. A novel access to 1,4-dialkyl- and 1,4-diaryl-2,3-dinitro-1,3-butadienes. Tetrahedron Lett 1990;31:4933–6.
[15] Dell'Erba C, Mele A, Novi M, Petrillo G, Stagnaro P. Synthetic exploitation of the ring-opening of 3,4-dinitrothiophene. Access to 1,4-disubstituted 2,3-dinitro-1,3-butadienes and 2,3-butanedione dioximes. Tetrahedron 1992;48:4407–18.
[16] Bianchi L, Dell'Erba C, Maccagno M, Morganti S, Petrillo G, Rizzato E, et al. Nitrobutadienes from β-nitrothiophenes: valuable building-blocks in the overall ring-opening/ring-closure protocol to homo- or hetero-cycles. Arkivoc 2006;(vii):169–85.
[17] Bianchi L, Maccagno M, Petrillo G, Sancassan F, Spinelli D, Tavani C. 2,3-Dinitro-1,3-butadienes: versatile building-blocks from the ring-opening of 3,4-dinitrothiophene. In: Attanasi OA, Spinelli D, editors. Targets in heterocyclic systems: chemistry and Properties, vol 10. Rome: Società Chimica Italiana; 2006. p. 1–23.
[18] Louie KG, Behrens BC, Kinsella TJ, Hamilton TC, Grotzinger KR, McKoy WM, et al. Radiation survival parameters of antineoplastic drug-sensitive and -resistant human ovarian cancer cell lines and their modification by buthionine sulfoximine. Cancer Res 1985;45:2110–5.

[19] Lieber M, Smith B, Szakal A, Nelson-Rees W, Todaro G. A continuous tumor-cell line from a human lung carcinoma with properties of type II alveolar epithelial cells. Int J Cancer 1976;17:62–70.
[20] Chen JY, Funk WD, Wright WE, Shay JW, Minna JD. Heterogeneity of transcriptional activity of mutant p53 proteins and p53 DNA target sequences. Oncogene 1993;8:2159–66.
[21] Akagi T, Kimoto T. Human cell line (HGC-27) derived from the metastatic lymph node of gastric cancer. Acta Med Okayama 1976;30:215–9.
[22] Tompkins WA, Watrach AM, Schmale JD, Schultz RM, Harris JA. Cultural and antigenic properties of newly established cell strains derived from adenocarcinomas of the human colon and rectum. J Natl Cancer Inst 1974;52:1101–10.
[23] Weiss A, Wiskocil RL, Stobo JD. The role of T3 surface molecules in the activation of human T cells: a two-stimulus requirement for IL 2 production reflects events occurring at a pre-translational level. J Immunol 1984;133:123–8.
[24] Cailleau R, Young R, Olive M, Reeves Jr WJ. Breast tumor cell lines from pleural effusions. J Natl Cancer Inst 1974;53:661–74.
[25] Zeuthen J, Norgaard JO, Avner P, Fellous M, Wartiovaara J, Vaheri A, et al. Characterization of a human ovarian teratocarcinoma-derived cell line. Int J Cancer 1980;25:19–23.
[26] Evans VJ, Larock JF, Yosida TH, Potter M. A new tissue culture isolation and explantation of the P388 lymphocytic neoplasm in a chemically characterized medium. Exp Cell Res 1963;32:212–7.
[27] Hussain RF, Nouri AME, Oliver RTD. A new approach for measurement of cytotoxicity using colorimetric assay. J Immunol Methods 1993;160:89–96.
[28] Coluccia M, Boccarelli A, Mariggiò MA, Cardellicchio N, Caputo P, Intini FP, et al. Platinum(II) complexes containing iminoethers: a trans platinum antitumour agent. Chem-Biol Interact 1995;98:251–66.
[29] Geske FJ, Gerschenson LE. The biology of apoptosis. Hum Pathol 2001;32:1029–38.
[30] Fulda S, Debatin KM. Modulation of apoptosis signaling for cancer therapy. Immunol Ther Exp (Warsz) 2006;54:173–5.
[31] Green AM, Steinmetz ND. Monitoring apoptosis in real time. Cancer J 2002;8:82–92.
[32] Gadducci A, Cosio S, Muraca S, Genazzani AR. Molecular mechanisms of apoptosis and chemosensitivity to platinum and paclitaxel in ovarian cancer: biological data and clinical implications. Eur J Gynaecol Oncol 2002;23:390–6.
[33] Gonzales VM, Fuertes MA, Alonso C, Perez JM. Is cisplatin-induced cell death always produced by apoptosis? Mol Pharmacol 2001;59:657–63.
[34] Schmidt S, Rainer J, Ploner C, Presul E, Riml S, Kofler R. Glucocorticoid-induced apoptosis and glucocorticoid resistance: molecular mechanisms and clinical relevance. Cell Death Differ 2004;11(Suppl. 1): S45–55.